A MODERN VIEW ON EXCLUSIVE REACTIONS: SELECTED TOPICS AT THE INTERFACE BETWEEN PERTURBATIVE AND NON-PERTURBATIVE QCD*

N.G. STEFANIS

Institut für Theoretische Physik II
Ruhr-Universität Bochum
D-44780 Bochum, Germany

(Received November 7, 1994)

A critical survey of recent developments in the description of exclusive reactions is given. An approach to nucleon distribution amplitudes and related properties is discussed, which makes use of QCD sum rules and the renormalization group. The behavior of helicity-conserving nucleon form factors in the spacelike region has been studied in detail, emphasizing the importance of a self-consistent treatment of endpoint contributions via a modified QCD factorization which takes into account Sudakov suppression of soft-gluon radiation. None of the considered observables is inconsistent with the data, although the leading perturbative contribution to the pion and nucleon form factors is small, calling for rather large K-factors and/or sizeable higher-twist contributions.

PACS numbers: 12.38. Bx, 12.38. Cy, 11.50. Li, 13.40. Gp

1. Preface

The prevalent theory of strong interactions at the microscopic level is Quantum Chromodynamics (QCD). It is believed that QCD has within it the power to predict the short-distance behavior of hadrons in terms of quark and gluon degrees of freedom, as well as to provide a dynamical explanation of quark confinement and the formation of hadronic bound states. Lack of precise knowledge about the interquark forces at large separation and the mathematical intractability of the nonlinear structure of the QCD dynamics preclude an *ab initio* analytical calculation of hadronic

* Presented at the XXXIV Cracow School of Theoretical Physics, Zakopane, Poland, June 1–10, 1994.

quantities. One has to resort to (more or less) plausible phenomenological confinement mechanisms or use frameworks which are capable of simulating the nonperturbative regime of QCD either in the continuum, *e.g.*, via QCD sum rules [1], or numerically on the gauge lattice [2]. Although lattice calculations in the strong-coupling domain are very promising [3], there are conceptual and technical limitations; *e.g.*, the properties of a single proton cannot be determined properly at present. More recent approaches attempt to simulate low-energy QCD by effective Lagrangians, *e.g.*, the Nambu-Jona-Lasinio model (for a recent review, see [4] and references cited therein), which implement chiral symmetry breaking and may, in principle, be derivable from QCD, albeit a rigorous derivation via path-integral techniques is still rudimentary. The perception of strong-interaction dynamics at different resolution (energy) scales is illustrated in Fig. 1.

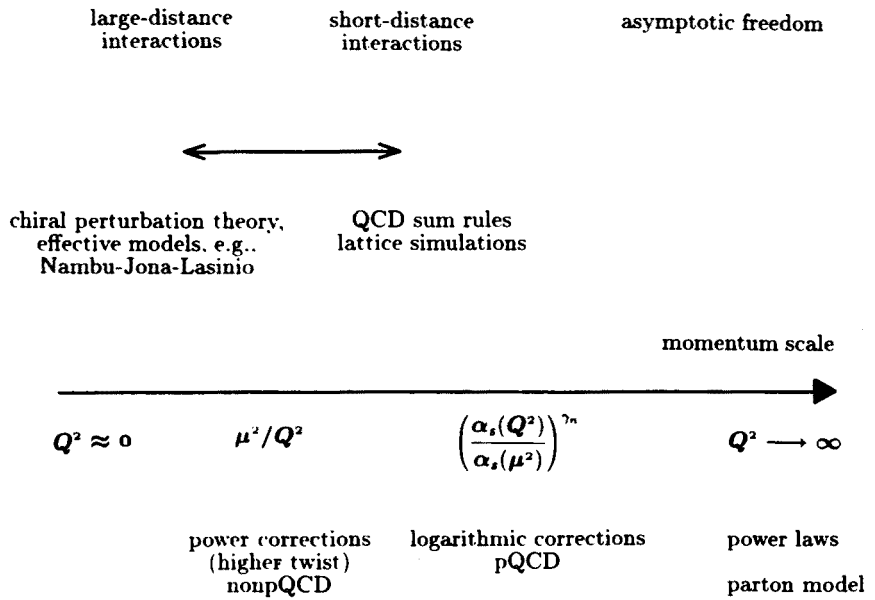

Fig. 1. "Flow" of strong-interactions dynamics.

1. Introduction

The quantitative description of exclusive reactions, in which *intact* hadrons appear in the initital and final states, involves the detailed calculation of hadronic wave functions — uncalculable within a perturbative framework. The theoretical basis in applying perturbative QCD is provided by the factorization theorem [5], which enables the multiplicative separation of

short- from large-distance interactions in a renormalizable way. In technical terms, this means that the process can be described by a Wilson operator product expansion (OPE) [6]. The c-number coefficient function (small-distance interaction) corresponds to a (process-dependent) hard-scattering amplitude which in leading order of the coupling constant is described by the one-gluon exchange kernel, the justification being provided by asymptotic freedom [7]. All information about the strong nonperturbative interactions at large distances is contained in the matrix elements of appropriate operators, describing the initial and final hadronic states. At leading twist level, these soft parts are represented by valence-state wave functions describing the distribution in longitudinal momentum fractions, truncated from above by a characteristic virtuality of the order of the factorization scale.

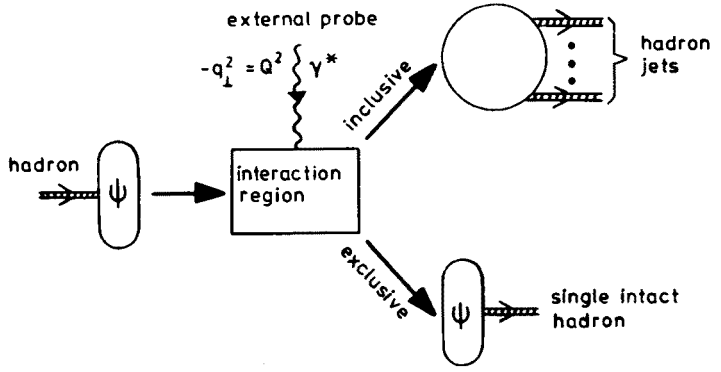

Fig. 2. Factorizition of short- and large-distance effects within QCD.

A convenient framework for describing exclusive reactions, based on factorization and the renormalization group, is the convolution scheme of Brodsky and Lepage [8] (see also [9, 10]). Within this scheme, the reaction amplitude becomes the product (the convolution) of two or more factors, each depending only on the dynamics specific for that particular momentum (or distance scale). The nonperturbative information on the hadronic quark structure is encapsulated in the distribution amplitude over longitudinal momentum fractions x_i (i = number of valence quarks), termed $\Phi(x_i, \mu^2)$, which is the integral over the transverse momenta $k_{\perp i}$ of the hadron valence-quark wave function at resolution scale μ^2 (see Fig. 2). In a physical gauge (like the light-cone gauge, $A^+ = 0$ — extensively used in [8]), it is the probability amplitude for the hadron to consist of valence quarks with fractional momenta $0 \leq x_i \leq 1$, $\sum_i x_i = 1$ (in a $p_3 \to \infty$ frame) moving collinearly up to the scale μ^2. The hadronic distribution amplitudes are *universal* quantities, *i.e.*, independent of the specific exclusive process considered. Their extraction directly from experiment is still a prodigious task, but may become feasible in the future [11, 12].

On the other hand, the short-distance or large-momentum transfer subprocesses are accounted for by the hard-scattering amplitude which is calculable within perturbative QCD. Contributions from higher Fock states with additional $q\bar{q}$-pairs and gluons are suppressed by powers of the momentum transfer. The principal success of this scheme is the predicted power-law fall-off behavior of elastic form factors at asymptotic (space-like) momentum transfer [8]. However, where the transition to the asymptotic regime takes place remains a point of controversy [13, 14].

3. On the nucleon distribution amplitude

For the discussion below, it is instructive to write the valence-quark component of the proton Fock state with positive helicity:

$$|P,+\rangle = \frac{1}{\sqrt{N_c!}} \int_0^1 [dx] \int [d^2k_\perp] \Big\{ \Psi_{123}\, \mathcal{M}^{a_1a_2a_3}_{+-+} + \Psi_{213}\, \mathcal{M}^{a_1a_2a_3}_{-++} - \Big(\Psi_{132} + \Psi_{231}\Big) \mathcal{M}^{a_1a_2a_3}_{++-} \Big\} \epsilon_{a_1a_2a_3}\,, \quad (1)$$

where we assume the proton to be moving rapidly in the 3-direction, meaning that the ratio of transverse to longitudinal momentum fractions of the quarks is small, and the subscripts on Ψ refer to the order of momentum arguments, for example, $\Psi_{123}(x, \vec{k}_\perp) = \Psi(x_1, \vec{k}_{\perp 1}; x_2, \vec{k}_{\perp 2}; x_3, \vec{k}_{\perp 3})$. The integration measures are defined as follows

$$\int_0^1 [dx] \equiv \int_0^1 dx_1 \int_0^{1-x_1} dx_2 \int_0^1 dx_3\, \delta(1 - x_1 - x_2 - x_3) \quad (2)$$

and

$$[d^2k_\perp] = \frac{1}{(16\pi^3)^2}\, \delta^{(2)}\left(\sum_{i=1}^3 \vec{k}_{\perp i}\right) d^2k_{\perp 1} d^2k_{\perp 2} d^2k_{\perp 3}\,. \quad (3)$$

The three-quark state with helicities $\lambda_1, \lambda_2, \lambda_3$ and colors a_1, a_2, a_3 is given by

$$\mathcal{M}^{a_1a_2a_3}_{\lambda_1\lambda_2\lambda_3} = \frac{1}{\sqrt{x_1x_2x_3}} |u_{a_1}; x_1, \vec{k}_{\perp 1}, \lambda_1\rangle |u_{a_2}; x_2, \vec{k}_{\perp 2}, \lambda_2\rangle |d_{a_3}; x_3, \vec{k}_{\perp 3}, \lambda_3\rangle\,. \quad (4)$$

Since the orbital angular momentum is assumed to be zero, the proton helicity is the sum of the quark helicities. The quark states are normalized by

$$\langle q_{a_i'}; x_i', \vec{k}'_{\perp i}\lambda_i' | q_{a_i}; x_i, \vec{k}_{\perp i}\lambda_i\rangle = 2x_i(2\pi)^3 \delta_{a_i'a_i} \delta_{\lambda_i'\lambda_i} \delta(x_i' - x_i) \delta(\vec{k}'_{\perp i} - \vec{k}_{\perp i})\,. \quad (5)$$

The nucleon distribution amplitude is defined by [8]

$$\Phi(x_i,\mu^2)=\left(\ln\frac{\mu^2}{\Lambda^2}\right)^{-\frac{3}{2}\gamma_F\beta}\int^{\mu^2}[d^2k_\perp]\,\psi(x_i,\vec{k}_\perp^{(i)})\,, \tag{6}$$

where the logarithm in front of the integral is due to wave function renormalization, *i.e.*, $Z_2=\lim_{\mu^2\to\infty}\left(\ln\frac{\mu^2}{\Lambda^2}\right)^{-\frac{3}{2}\gamma_F\beta}$, β is the Gell-Mann and Low function, and γ_F is the anomalous dimension associated with quark self energy. The physical content of Eq. (6) is that an external probe, for example, an off-shell photon, "sees" only the distribution of quarks over longitudinal momenta inside the nucleon, while its transverse size requires wavelengths $\propto 1/\mu$, so that the distribution of quarks over transverse momenta is not resolved.

The nucleon distribution amplitude is related to the following trilocal matrix element of three-quark operators between the vacuum and the nucleon, covariantly parametrized in terms of the scalar functions $V=$ (vector), $A=$ (axial vector), and $T=$ (tensor) with positive parity [15]:

$$\begin{aligned}\left\langle 0|u_\alpha^{a_1}(z_1)u_\beta^{a_2}(z_2)d_\gamma^{a_3}(z_3)|p\right\rangle\epsilon_{a_1a_2a_3}=\\ \tfrac{1}{4}f_N\Big[(\not{p}C)_{\alpha\beta}(\gamma_5N)_\gamma V(z_i\cdot p)+(\not{p}\gamma_5C)_{\alpha\beta}N_\gamma A(z_i\cdot p)\\ -(\sigma_{\mu\nu}p_\nu C)_{\alpha\beta}(\gamma_\mu\gamma_5N)_\gamma T(z_i\cdot p)\Big]\,.\end{aligned} \tag{7}$$

In (7), $\not{p}=p_\mu\gamma_\mu$, $\sigma_{\mu\nu}=\frac{1}{2}[\gamma_\mu,\gamma_\nu]$, N stands for the proton spinor, C denotes the charge conjugation matrix, and the proton state with momentum p is notated $|p\rangle$. The dimensionful constant f_N represents the value of the proton wave function at the origin of the configuration space, *i.e.*, at zero interquark separation.

Because of the permutation symmetry between the two up quarks, the functions V and T are symmetric and A antisymmetric in their first two arguments. In addition, the requirement that the three quarks have to be coupled to give an isospin $\frac{1}{2}$ state (the nucleon), yields the relation

$$2T(1,2,3)=V(1,3,2)-A(1,3,2)+V(2,3,1)-A(2,3,1)\,. \tag{8}$$

Hence, it follows that Eq. (1) can be expressed in terms of a single independent scalar function, *e.g.*, [16] $\Phi_N(x_i)=V(x_i)-A(x_i)$, which transforms under the two-dimensional matrix representation of the permutation group and has the normalization

$$\int_0^1[dx]\,\Phi_N(x_i,\mu)=1\,. \tag{9}$$

Although $\psi(x_i, \vec{k}_{\perp i})$, and hence $\Phi(x_i, Q^2)$, cannot be calculated within perturbative QCD, an evolution equation with respect to the momentum scale can be derived on the basis of the renormalization group equation (RGE) [8], so that

$$\left\{ Q^2 \frac{\partial}{\partial Q^2} + \frac{3C_F}{2\beta} \right\} \Phi(x_i, Q^2) = \frac{C_B}{\beta} \int_0^1 [dy]\, V(x_i, y_i)\, \Phi(y_i, Q^2)\,, \qquad (10)$$

where C_F and C_B are, respectively, the Casimir operators of the fundamental and adjoint representations of SU(3). The one-gluon-exchange kernel V at the Born level has been calculated in [8].

Any solution of this equation can be expressed in terms of the evolution-kernel eigenfunctions $\tilde{\Phi}_n$ and the asymptotic distribution amplitude [8]

$$\Phi_{\rm as}(x_i) = 120 x_1 x_2 x_3 \qquad (11)$$

to read

$$\Phi(x_i, Q^2) = \Phi_{\rm as}(x_i) \sum_{n=0}^{\infty} B_n(\mu^2) \exp\left(\int_{\mu^2}^{Q^2} \frac{d\bar{\mu}}{\bar{\mu}} \gamma_F(g(\bar{\mu}^2)) \right) \tilde{\Phi}_n(x_i)\,, \qquad (12)$$

where the projection coefficients

$$B_n(\mu^2) = \frac{N_n}{120} \int_0^1 [dx] \tilde{\Phi}_n(x_i) \Phi_N(x_i, \mu^2) \qquad (13)$$

depend on the nucleon wave function itself and are therefore uncalculable within perturbative QCD. In contrast, its momentum-scale dependence is RG-controlled and in leading log approximation one has

$$B_n(Q^2) = B_n(\mu^2) \left(\frac{\ln \frac{Q^2}{\Lambda^2_{\rm QCD}}}{\ln \frac{\mu^2}{\Lambda^2_{\rm QCD}}} \right)^{-\gamma_n}. \qquad (14)$$

The eigenfunctions $\{\tilde{\Phi}_n\}$ and the asymptotic wave function $\Phi_{\rm as}$ [17] are completely determined by perturbative QCD. In the case of the meson, $\Phi_{\rm as} = {}^3\!/_4(1-\zeta^2)$ with $\zeta = x_1 - x_2$, and the system of multiplicatively renormalizable (conformal) operators is represented by the Gegenbauer polynomials $C_n^{3/2}(\zeta)$ [18], which are orthogonal with respect to the weight $(1-\zeta^2)$.

Within this basis, the anomalous dimension matrix diagonalizes and the corresponding eigenvalues can be calculated in closed form [19, 20].

The nucleon case is more complicated because the orthogonality condition

$$\int_0^1 [dx]\, x_1 x_2 x_3 \tilde{\Phi}_k(x_i)\tilde{\Phi}_l(x_i) = N_k^{-1}\delta_{kl} \tag{15}$$

is insufficient to determine the polynomial basis uniquely. This is because the orthogonalization of polynomials depending on two (or more) variables via a generalization of the Hilbert–Schmidt method has no unique solution. A polynomial basis orthogonal with respect to the weight $w(x_i) = x_1 x_2 x_3$ is provided by the Appell polynomials [18]. Hence, it is convenient to expand the nucleon eigenfunctions $\{\tilde{\Phi}_n\}$ in terms of these polynomials [8]:

$$\tilde{\Phi}_k(x_i) = \sum_{n,m=0}^{n+m=M} c_{nm}^k \mathcal{F}_{nm}(5,2,2;x_1,x_2)\,. \tag{16}$$

However, the explicit construction of nucleon eigenfunctions beyond polynomial order $M = 2$ becomes increasingly tedious and the corresponding eigenvalues

$$\gamma_n = \left(\frac{3}{2}\frac{C_F}{\beta} + 2\eta_n \frac{C_B}{\beta}\right), \tag{17}$$

(where η_n are the zeros of the characteristic polynomial that diagonalizes the evolution kernel) of the anomalous dimension matrix are no longer rational numbers. In recent meetings [21–23], we reported on a calculation [24] of $\{\tilde{\Phi}_n\}$ which makes use of symmetrized Appell polynomials

$$\tilde{\mathcal{F}}_{mn}(x_1,x_3) = \tfrac{1}{2}[\mathcal{F}_{mn}(x_1,x_3) \pm \mathcal{F}_{nm}(x_1,x_3)]\,, \tag{18}$$

(where $+$ refers to $m \geq n$ and $-$ to $m < n$) of up to maximum degree $M = 9$. The advantage of this basis over the ordinary one is that the integral operator $\hat{V} \equiv \int_0^1 [dy]\, V(x_i,y_i)$ commutes with the permutation operator P_{13} and thus becomes block-diagonal within a particular polynomial order for different symmetry classes ($S_n = \pm 1$) of eigenfunctions. Then it is possible to analytically diagonalize $\hat{V}$ up to order 7. For every order M, there are $M+1$ eigenfunctions of the same order with an excess of symmetric terms by one for even orders. The total number of eigenfunctions up to order M is $\#_{\max}(M) = {}^1\!/_2(M+1)(M+2)$ and the corresponding $(M+1)$ eigenvalues are obtained by diagonalizing the $(M+1)\times(M+1)$ matrix. The pattern of three-quark anomalous dimensions up to order $M = 9$ is shown in Fig. 3.

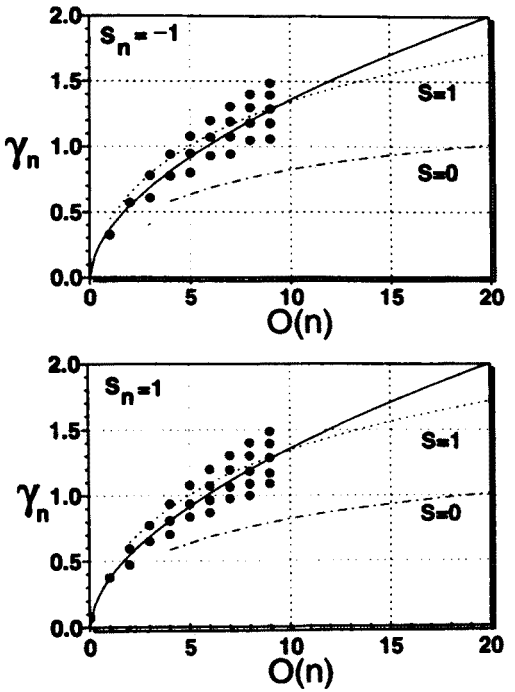

Fig. 3. Pattern of nucleon-kernel eigenvalues (three-quark anomalous dimensions) up to order $M = 9$. There are 30 symmetric and 25 antisymmetric eigenfunctions under the permutation P_{13}, shown in comparison with the eigenvalues of the meson kernel.

It turns out that the system of eigenfunctions $\{\tilde{\Phi}_k\}$ satisfies a commutative algebra subject to the triangular condition $|\mathcal{O}(k) - \mathcal{O}(l)| \leq \mathcal{O}(m) \leq \mathcal{O}(k) + \mathcal{O}(l)$:

$$\tilde{\Phi}_k(x_i)\tilde{\Phi}_l(x_i) = \sum_{m=0}^{\infty} F_{kl}^m \tilde{\Phi}_m(x_i) \tag{19}$$

with structure coefficients F_{kl}^m defined by

$$F_{kl}^m = N_m \int_0^1 [dx]\, x_1 x_3 (1 - x_1 - x_3) \tilde{\Phi}_m(x_i)\tilde{\Phi}_k(x_i)\tilde{\Phi}_l(x_i)\,. \tag{20}$$

These structure coefficients are symmetric, *i.e.*, $F_{kl}^m = F_{lk}^m$. Furthermore, $F_{kk}^0 = N_0/N_k$. The utility of this algebra for concrete applications will be discussed elsewhere. The eigenvalues γ_n of the diagonalized evolution equation coincide with the anomalous dimensions of multiplicatively renormalizable $I_{1/2}$ baryonic operators of twist three (recall that twist = dimension

– spin). Because they are positive fractional numbers increasing with M, higher-order terms in (12) are gradually suppressed.

An orthogonalized basis including a total of 55 eigenfunctions (polynomial order $M = 9$) together with the associated normalization coefficients and anomalous dimensions has been constructed in [24]. A compedium of the results up to order $M = 4$ is given in Table I.

TABLE I

Orthogonal eigenfunctions $\tilde{\Phi}_n(x_i) = \sum_{lk} a^n_{kl}\, x_1^k x_3^l$ of the nucleon evolution equation up to polynomial order $M = 4$ in terms of the coefficient matrix a^n_{kl} with $a^n_{kl} = S_n\, a^n_{lk}$, and $a^n_{22} = 0$ for all n. The numerical results for $n \geq 12$ have been obtained with a much higher numerical accuracy than shown in the table.

n	M	S_n	γ_n	η_n	N_n
0	0	1	$\frac{2}{27}$	-1	120
1	1	-1	$\frac{26}{81}$	$\frac{2}{3}$	1260
2	1	1	$\frac{10}{27}$	1	420
3	2	1	$\frac{38}{81}$	$\frac{5}{3}$	756
4	2	-1	$\frac{46}{81}$	$\frac{7}{3}$	34020
5	2	1	$\frac{16}{27}$	$\frac{5}{2}$	1944
6	3	1	$\frac{115-\sqrt{97}}{162}$	$\frac{-(-79+\sqrt{97})}{24}$	$\frac{4620\,(485+11\sqrt{97})}{97}$
7	3	1	$\frac{115+\sqrt{97}}{162}$	$\frac{79+\sqrt{97}}{24}$	$\frac{4620\,(485-11\sqrt{97})}{97}$
8	3	-1	$\frac{559-\sqrt{4801}}{810}$	$\frac{-(-379+\sqrt{4801})}{120}$	$\frac{27720\,(33607-247\sqrt{4801})}{4801}$
9	3	-1	$\frac{559+\sqrt{4801}}{810}$	$\frac{379+\sqrt{4801}}{120}$	$\frac{27720\,(33607+247\sqrt{4801})}{4801}$
10	4	-1	$\frac{346-\sqrt{1081}}{405}$	$\frac{-(-256+\sqrt{1081})}{60}$	$\frac{196560\,(7567-13\sqrt{1081})}{1081}$
11	4	-1	$\frac{346+\sqrt{1081}}{405}$	$\frac{256+\sqrt{1081}}{60}$	$\frac{196560\,(7567+13\sqrt{1081})}{1081}$
12	4	1	0.70204	3.23876	1
13	4	1	0.80651	3.94397	1
14	4	1	0.93589	4.81727	1

TABLE I continued

n	a_{00}^n	a_{10}^n	a_{20}^n	a_{11}^n	a_{30}^n
0	1	0	0	0	0
1	0	1	0	0	0
2	-2	3	0	0	0
3	2	-7	8	4	0
4	0	1	$-\frac{4}{3}$	0	0
5	2	-7	$\frac{14}{3}$	14	0
6	1	-6	$\frac{41+\sqrt{97}}{4}$	$\frac{3\left(31-\sqrt{97}\right)}{4}$	$\frac{-5\left(17+\sqrt{97}\right)}{16}$
7	1	-6	$\frac{41-\sqrt{97}}{4}$	$\frac{3\left(31+\sqrt{97}\right)}{4}$	$\frac{-5\left(17-\sqrt{97}\right)}{16}$
8	0	1	-3	0	$\frac{601+\sqrt{4801}}{264}$
9	0	1	-3	0	$\frac{601-\sqrt{4801}}{264}$
10	0	1	-5	0	$\frac{379+\sqrt{1081}}{48}$
11	0	1	-5	0	$\frac{379-\sqrt{1081}}{48}$
12	153.37061	-1380.33552	5232.86956	5006.42414	-8063.85349
13	332.500864	-2992.50778	9240.51876	17166.06044	-11695.76593
14	-137.11538	1234.03849	-1843.05428	-12981.41464	-587.61051

TABLE I continued

n	a_{21}^n	a_{40}^n	a_{31}^n	a_{22}^n
0	0	0	0	0
1	0	0	0	0
2	0	0	0	0
3	0	0	0	0
4	0	0	0	0
5	0	0	0	0
6	$\frac{-5\left(31-\sqrt{97}\right)}{8}$	0	0	0
7	$\frac{-5\left(31+\sqrt{97}\right)}{8}$	0	0	0
8	$\frac{59-\sqrt{4801}}{44}$	0	0	0
9	$\frac{59+\sqrt{4801}}{44}$	0	0	0
10	$\frac{61-\sqrt{1081}}{8}$	$\frac{-\left(159+\sqrt{1081}\right)}{40}$	$\frac{-\left(61-\sqrt{1081}\right)}{8}$	0
11	$\frac{61+\sqrt{1081}}{8}$	$\frac{-\left(159-\sqrt{1081}\right)}{40}$	$\frac{-\left(61+\sqrt{1081}\right)}{8}$	0
12	-9178.44426	4345.63139	4926.80699	8503.27454
13	-31471.11081	5068.49438	19489.65169	23962.91822
14	23799.26017	1382.85660	-10302.90296	-26992.71442

The nonperturbative input enters Eq. (12) through the coefficients $B_n(\mu^2)$ which represent nonperturbative matrix elements of appropriate three-quark operators (in the Fock–Schwinger gauge $x_\mu A_\mu = 0$) interpolating between the proton and the vacuum. Their determination involves correlators of the form [16, 25, 26]

$$I^{(n_1n_2n_3,m)}(q,z) = i\int d^4x\, e^{iq\cdot x}\langle\Omega|T\big(O_\gamma^{(n_1n_2n_3)}(0)\hat{O}_{\gamma'}^{(m)}(x)\big)|\Omega\rangle(z\cdot\gamma)_{\gamma\gamma'}$$

$$= (z\cdot q)^{n_1+n_2+n_3+m+3} I^{(n_1n_2n_3,m)}(q^2)\,, \qquad (21)$$

where z is a lightlike auxiliary vector ($z^2 = 0$) and the factor $(z\cdot\gamma)_{\gamma\gamma'}$ serves to project out the leading-twist structure of the correlator. The computation of the Wilson coefficients on the quark side of the correlator amounts to the perturbative evaluation of diagrams involving quark/gluon condensates [16]. It yields the theoretical side of the sum rule. The hadronic (phenomenological) side of the sum rule is obtained by saturating the correlator by the lowest-mass baryon state(s) via a dispersion relation. Reconciliation of the two sides of the sum rule with respect to the Borel parameter (which resembles momentum) determines the margin of permissible values for a particular moment (for more details, see [16, 29]). The three-quark operators in Eq. (21) are typified by the expression

$$O^{(n_1n_2n_3)} = (z\cdot p)^{-(n_1+n_2+n_3)}\prod_{i=1}^{3}\left(iz\cdot\frac{\partial}{\partial z_i}\right)^{n_i} O(z_i\cdot p)\big|_{z_i=0}\,. \qquad (22)$$

Their matrix elements

$$\langle\Omega|O_\gamma^{(n_1n_2n_3)}(0)|P(p)\rangle = f_N(z\cdot p)^{n_1+n_2+n_3+1} N_\gamma\, O^{(n_1n_2n_3)} \qquad (23)$$

are related to the moments

$$O^{(n_1n_2n_3)} = \int_0^1 [dx] x_1^{n_1}x_2^{n_2}x_3^{n_3} O(x_1,x_2,x_3)\,, \qquad (24)$$

where $O(x_i)$ stands for one of the amplitudes V, T, A, or linear combinations of them. Because of the linear momentum conservation, $x_1+x_2+x_3 = 1$, not all the moments at a given order $M = n_1+n_2+n_3$ are linearly independent. For instance, at order $M = 3$ there are 20 moments out of which only 10 are strict. Which combinations are actually taken, depends on the choice of the polynomial basis in which the eigenfunctions are expressed. In the

present work, we follow [8] to use as such the powers of the mononomial $x_1 x_3$. Then

$$\Phi_N^{(i0j)} = \int_0^1 [dx]\, x_1^i\, x_2^0\, x_3^j\, \Phi_N(x_k, \mu^2)\,. \tag{25}$$

As we first pointed out in [21–23], it is possible to derive a *closed-form* expression of the expansion coefficients B_n in terms of strict moments, an expression which enables the *analytical* calculation of these coefficients to any desired order of polynomial expansion:

$$\frac{B_n(\mu^2)}{\sqrt{N_n}} = \frac{\sqrt{N_n}}{120} \sum_{i,j=0}^{\infty} a_{ij}^n\, \Phi^{(i0j)}(\mu^2)\,. \tag{26}$$

The projection coefficients a_{ij}^n and the normalization constants N_n up to order $M = 9$ have been calculated in [24]. Those up to order $M = 4$ are shown in Table I. The utility of Eq. (26) is twofold. First, as we shall see below, the moments of hadron distribution amplitudes are not accurately determined. Thus, without the *explicit* relation between expansion coefficients and strict moments, one has to perform a simultaneous and self-consistent fit to the moment constraints, which becomes increasingly tedious as the moment-order grows. Second, as already stated above, the orthogonalization procedure of polynomials with more than one variable is not unique. This means that in order to compare expansion coefficients B_n, obtained in different approaches, they ought to be *normalized*. Without the knowledge of the normalization constants N_n, the values of B_n are of no significance. However, having derived Eq. (26), the knowledge of the normalization used in different approaches becomes superfluous. The coefficients B_n can be self-consistently computed on the basis of the strict moments only which are universal quantities, modulo normalization. (Recall that, following [16], $\Phi_N^{(000)} = 1$.) All these advantages will become apparent below.

The link between B_n and the strict moments of Φ_N is exemplified below (see also [27, 28]).

$$\begin{aligned}
B_1(\mu^2) =& \frac{1260}{120}\left[\Phi_N^{(100)} - \Phi_N^{(001)}\right]\Big|_{\mu^2}\,,\\
B_2(\mu^2) =& \frac{420}{120}\left[2\Phi_N^{(000)} - 3\Phi_N^{(100)} - 3\Phi_N^{(001)}\right]\Big|_{\mu^2}\,,\\
B_3(\mu^2) =& \frac{756}{120}\left[2\Phi_N^{(000)} - 7\Phi_N^{(100)} - 7\Phi_N^{(001)} + 8\Phi_N^{(200)}\right.\\
&\left. + 4\Phi_N^{(101)} + 8\Phi_N^{(002)}\right]\Big|_{\mu^2}\,,
\end{aligned}$$

$$B_4(\mu^2) = \frac{34020}{120}\left[\Phi_N^{(100)} - \Phi_N^{(001)} - \frac{4}{3}\Phi_N^{(200)} + \frac{4}{3}\Phi_N^{(002)}\right]\Big|_{\mu^2},$$

$$B_5(\mu^2) = \frac{1944}{120}\left[2\Phi_N^{(000)} - 7\Phi_N^{(100)} - 7\Phi_N^{(001)} + \frac{14}{3}\Phi_N^{(200)} + 14\Phi_N^{(101)} + \frac{14}{3}\Phi_N^{(002)}\right]\Big|_{\mu^2}. \tag{27}$$

Note that B_0 is fixed to unity by the normalization of Φ_N (*cf.*, Eq. (9)). Furthermore, note that in the present work the notations of [29] are adopted, which imply that B_2 has the reversed sign relative to [8] and is given by

$$B_2(\mu^2) = \frac{420}{120}\left[\Phi_N^{(000)} - 3\Phi_N^{(010)}\right]\Big|_{\mu^2}. \tag{28}$$

Useful constraints on the nucleon distribution amplitude are obtained implicitly by restricting its first few moments within intervals determined from QCD sum rules adapted to the light-cone [16, 25, 26].These are evaluated with the aid of correlators of the type (21) at some self-consistently determined normalization point $\mu_0 = \mu_F$ of order 1 GeV (see, *e.g.*, [29]) at which a short-distance OPE can be safely performed and quark-hadron duality is supposed to be valid. The original Chernyak-Zhitnitsky (CZ) approach [16] has been rectified in the analysis of King and Sachrajda (KS) [25], and has more recently been extended to provide sum-rule constraints for the third-order moments by Chernyak, Ogloblin, and Zhitnitsky (COZ) [26]. The new set of moment sum rules comprises 18 nontrivial terms with restricted margins that comply with most of the previous results [16, 25], but disagree with those derived on the lattice for the lowest two moments [30, 31].

The constraints on the moments have been used by several authors [16, 25, 26, 32] to (re-)construct model amplitudes for the nucleon which, being the product of a fitting procedure, do not necessarily satisfy all sum-rule requirements. We reiterate that only the knowledge of Eq. (26) makes it possible to determine analytically a genuine solution (if any exists) to the QCD sum rules. Of course, the problem of determining an unknown (even non-negative) distribution from a *finite* set of moments has no unique solution (see, *e.g.*, [29]) and references cited therein). Operationally, this means that the expansion in terms of eigenfunctions is truncated after taking into account bilinear combinations of longitudinal momentum fractions (two-quark correlations) and assuming that still higher-order terms are of minor importance, if properly included. Indeed, it was shown in [33] that deliberately incorporating in the decomposition of the distribution amplitude Appell polynomials after the second order renders the expansion ambiguous,

leading to either unphysical form factors or, if the right magnitude of the proton magnetic form factor is inputted, to unphysical oscillations of the distribution amplitude at small x-values. In the same work it was appreciated that imposing a "smoothening" criterion on such candidate solutions, is tantamount to reducing the third-order contributions to small corrections of the second-order solutions. This indicates clearly that the truncation at the second order is justifiable, since the shape of the corresponding amplitudes is a characteristic property of the *entire* series and that the errors (and amount of cut-off dependence involved) are of subleading importance. In some sense such a procedure resembles the optimization of the renormalization scheme dependence which aims at minimizing the next-to-leading order corrections, according to the *principle of minimum sensitivity* [34]. Physically, this truncated representation of the distribution amplitude can be thought of in analogy to a holographic image that is not destroyed when cut into smaller pieces (corresponding to a lower order of truncation) but becomes rather less sharp [27].

The moments of the amplitude Φ_N in terms of the coefficients B_n up to order $M = 3$ are displayed in Table II.

TABLE II

Moments of the nucleon distribution amplitude $\Phi_N^{(n_1 n_2 n_3)} \equiv \Phi_N^{[k]}$ in terms of the expansion coefficients B_n up to order $M = n_1 + n_2 + n_3 = 3$.

k	$\Phi_N^{[k]}$	Moments
0	$\Phi_N^{(000)}$	B_0
1	$\Phi_N^{(100)}$	$\frac{7B_0+B_1+B_2}{21}$
2	$\Phi_N^{(010)}$	$\frac{7B_0-2B_2}{21}$
3	$\Phi_N^{(001)}$	$\frac{7B_0-B_1+B_2}{21}$
4	$\Phi_N^{(200)}$	$\frac{108B_0+27B_1+27B_2+9B_3-B_4-B_5}{756}$
5	$\Phi_N^{(020)}$	$\frac{18B_0-9B_2+B_3+B_5}{126}$
6	$\Phi_N^{(002)}$	$\frac{108B_0-27B_1+27B_2+9B_3+B_4-B_5}{756}$
7	$\Phi_N^{(110)}$	$\frac{72B_0+9B_1-9B_2-3B_3+B_4-3B_5}{756}$
8	$\Phi_N^{(101)}$	$\frac{36B_0+9B_2-3B_3+2B_5}{378}$
9	$\Phi_N^{(011)}$	$\frac{72B_0-9B_1-9B_2-3B_3-B_4-3B_5}{756}$
10	$\Phi_N^{(300)}$	$\frac{87120B_0+29040B_1+29040B_2+17424B_3-1936B_4-1936B_5-33B_6-33\sqrt{97}B_6}{1219680}$ $\frac{-33B_7+33\sqrt{97}B_7+146B_8+2\sqrt{4801}B_8+146B_9-2\sqrt{4801}B_9}{1219680}$

TABLE II continued

k	$\Phi_N^{[k]}$	Moments
11	$\Phi_N^{(030)}$	$\frac{165\,B_0-110\,B_2+22\,B_3+22\,B_5+B_6+B_7}{2310}$
12	$\Phi_N^{(003)}$	$\frac{87120\,B_0-29040\,B_1+29040\,B_2+17424\,B_3+1936\,B_4-1936\,B_5}{1219680}$
		$\frac{-33\,B_6-33\sqrt{97}\,B_6-33\,B_7+33\sqrt{97}\,B_7-146\,B_8-2\sqrt{4801}\,B_8-146\,B_9+2\sqrt{4801}\,B_9}{1219680}$
13	$\Phi_N^{(210)}$	$\frac{5940\,B_0+1320\,B_1+88\,B_4-440\,B_5+15\,B_6+3\sqrt{97}\,B_6+15\,B_7-3\sqrt{97}\,B_7-12\,B_8-12\,B_9}{166320}$
14	$\Phi_N^{(201)}$	$\frac{130680\,B_0+14520\,B_1+43560\,B_2-8712\,B_3-968\,B_4+10648\,B_5}{3659040}$
		$\frac{-231\,B_6+33\sqrt{97}\,B_6-231\,B_7-33\sqrt{97}\,B_7-174\,B_8-6\sqrt{4801}\,B_8-174\,B_9+6\sqrt{4801}\,B_9}{3659040}$
15	$\Phi_N^{(120)}$	$\frac{495\,B_0+55\,B_1-165\,B_2-11\,B_3+11\,B_4-11\,B_5-3\,B_6-3\,B_7+B_8+B_9}{13860}$
16	$\Phi_N^{(102)}$	$\frac{130680\,B_0-14520\,B_1+43560\,B_2-8712\,B_3+968\,B_4+10648\,B_5}{3659040}$
		$\frac{-231\,B_6+33\sqrt{97}\,B_6-231\,B_7-33\sqrt{97}\,B_7+174\,B_8+6\sqrt{4801}\,B_8+174\,B_9-6\sqrt{4801}\,B_9}{3659040}$
17	$\Phi_N^{(021)}$	$\frac{495\,B_0-55\,B_1-165\,B_2-11\,B_3-11\,B_4-11\,B_5-3\,B_6-3\,B_7-B_8-B_9}{13860}$
18	$\Phi_N^{(012)}$	$\frac{5940\,B_0-1320\,B_1-88\,B_4-440\,B_5+15\,B_6+3\sqrt{97}\,B_6+15\,B_7-3\sqrt{97}\,B_7+12\,B_8+12\,B_9}{166320}$

The profile of the model amplitudes CZ, KS, COZ is similar and shows a strong asymmetry in the distribution over longitudinal momentum, with an up quark carrying most of the nucleon's momentum, whereas the other two quarks are "wee" (see [27]). Significantly, all these amplitudes predict a rather large ratio of the nucleon magnetic form factors $|G_M^n|/G_M^p \leq 0.5$.

An alternative nucleon distribution amplitude was proposed by Gari and Stefanis (GS) [32], which was motivated by the possibility of analyzing the form-factor data under the assumption that the electron-neutron differential cross section σ_n is dominated by G_E^n, whereas G_M^n is asymptotically small, or equivalently that $|F_1^n| \ll |F_2^n|$ at all Q^2 values. This model, which cannot match the sum-rule requirements in the allowed saturation range [29], predicts a different, though still asymmetric, longitudinal momentum balance than models of the CZ/COZ-type. In particular, it seems to indicate [29] strong two-quark correlations (diquarks [35]) inside the nucleon.

On the phenomenological side, all discussed models concur in predicting the right normalization and evolution behavior of the magnetic proton form factor [27, 29, 36], in fair agreement with the latest high-Q^2 SLAC data [37]. On the other hand, the quality of the current neutron data [38, 39] cannot provide conclusive evidence towards either one of these options.

The relationships between form factors for various exclusive reactions involving nucleons were explored in [29, 40] in which it was pointed out that the leading electromagnetic $N-\Delta^+$ transition form factor G_M^* [41] and the neutron magnetic form factor G_M^n are intrinsically anti-correlated via the

nucleon distribution amplitude. As a result, one of those form factors tends to be large when the other is small. Nucleon distribution amplitudes of the CZ-type lead to an almost vanishing G_M^*, whereas the GS one gives $|G_M^*|$ of the same order of magnitude as G_M^p. The first behavior would explain why the data on the ratio of the multipole amplitudes F_{E_2}/F_{M_1} yields a value compatible with zero. In contrast, the second one conforms to what one typically sees experimentally for other nucleon-resonance transitions [42]. These results were obtained by modeling the Δ distribution amplitude in an approximate way, namely, as being the symmetric part of the nucleon distribution amplitude. However, when more realistic model amplitudes for the Δ [43, 44] are used [45, 46], the sign of G_M^*, calculated with the GS-amplitude, turns out to be negative.

Substantial information about the nucleon's internal structure can be extracted from exclusive decays of heavy quarkonia into $p\bar{p}$. Recently, decays of several charmonium states have been measured by the E760 Collaboration at Fermilab with a remarkable degree of accuracy [47]. It was pointed out in [48] that the GS model leads to a prediction for the ${}^3S_1 \to p\bar{p}$ decay width, which is, at least, 50 times smaller (depending on the value of α_s actually used) than the experimental value. Thus, none of the models discussed so far is best for all the data while reasonably complying with the QCD sum-rule constraints.

However, physical intuition suggests a way to resolve these problems. The idea is the following. Suppose that COZ-type and GS-type solutions are not *mutually excluding* options for modeling the quark structure of the nucleon, but rather *complementary* to each other. This would imply that they are different facets of a more fundamental structure which is capable of unifying both types of models into a single one. We have shown in Ref. [45] that such a solution indeed exists and it turns out to be something of a hybrid between the COZ-amplitude and the GS one; thus the "heterotic" solution (Fig. 4). ("Heterosis" means increased vigor due to crossbreeding.)

To put this model in perspective, it predicts results in agreement with the data for a number of exclusive processes without resorting to any *ad hoc* tuning of the model parameters, like $\Lambda_{\rm QCD}$ or α_s from case to case. As a result, it provides the possibility of analyzing the form-factor data under the assumption that asymptotically $|G_M^n|/G_M^p \leq 0.1$, as in the case of the GS model, while the agreement with the QCD sum-rule requirements [26] on the moments of Φ_N up to order three has almost the same overall accuracy as in the case of the COZ model. It is remarkable that up to the second order, the heterotic amplitude satisfies the KS moment constraints better than the COZ amplitude (Table III). This is particularly important because the KS results have been independently verified by Carlson and Poor [43] and also by Bonekamp [49]. Furthermore, the calculated decay widths and

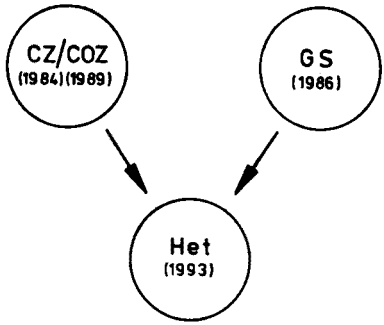

Fig. 4. Heterotic conception of the nucleon distribution amplitude: the heterotic model amalgamates the two previous types of models into a new structure with distinct geometrical characteristics by inherently combining their best features.

branching ratios for the decays of the charmonium states $^3S_1$, $^3P_1$, and $^3P_2$ into $p\bar{p}$ are in excellent agreement with the data [50].

TABLE III

Moments $M = n_1 + n_2 + n_3 \leq 3$ of the heterotic nucleon distribution amplitude in comparison with previous models and the QCD sum-rule constraints of Chernyak, Ogloblin, and Zhitnisky [26], and King and Sachrajda [25].

$(n_1 n_2 n_3)$	COZ-SR	KS-SR	$\Phi_{N/\mathrm{het}}^{(n_1 n_2 n_3)}$	$\Phi_{N/\mathrm{COZ}}^{(n_1 n_2 n_3)}$	$\Phi_{N/\mathrm{GS}}^{(n_1 n_2 n_3)}$	$\Phi_{N/\mathrm{KS}}^{(n_1 n_2 n_3)}$
(000)	1	1	1	1	1	1
(100)	0.540 – 0.620	0.46 – 0.59	0.5721	0.5790	0.6269	0.5500
(010)	0.180 – 0.200	0.18 – 0.21	0.1837	0.1920	0.1371	0.2100
(001)	0.200 – 0.250	0.22 – 0.26	0.2442	0.2290	0.2359	0.2400
(200)	0.320 – 0.420	0.27 – 0.37	0.3380	0.3690	0.2879	0.3500
(020)	0.065 – 0.088	0.08 – 0.09	0.0661	0.0680	0.0321	0.0900
(002)	0.090 – 0.120	0.10 – 0.12	0.1696	0.0890	0.0079	0.1200
(110)	0.080 – 0.100	0.08 – 0.10	0.1386	0.0970	0.1080	0.1000
(101)	0.090 – 0.110	0.09 – 0.11	0.0955	0.1130	0.2309	0.1000
(011)	−0.030 – 0.030	unreliable	−0.0210	0.0270	−0.0029	0.0200
(300)	0.210 – 0.250		0.2101	0.2445	0.1281	0.2333
(030)	0.028 – 0.040		0.0392	0.0381	0.0169	0.0573
(003)	0.048 – 0.056		0.1392	0.0485	−0.0515	0.0813
(210)	0.041 – 0.049		0.0789	0.0587	0.0463	0.0593
(201)	0.044 – 0.055		0.0490	0.0658	0.1135	0.0573
(120)	0.027 – 0.037		0.0504	0.0243	0.0278	0.0300
(102)	0.037 – 0.043		0.0372	0.0331	0.0836	0.0320
(021)	−0.004 – 0.007		−0.0235	0.0056	−0.0127	0.0027
(012)	−0.005 – 0.008		−0.0068	0.0073	−0.0241	0.0067

What's more, a whole spectrum of solutions conforming with the existing sets of sum rules [25, 26], all theoretically acceptable, was determined

in [28, 51]. This is achieved by recourse to a "hierarchical" treatment of the sum rules [28, 45, 51] that accounts for the higher stability of the lower-level moments relative to the higher ones [29] and does not overestimate the significance of the still unverified constraints [26] for the third-order moments. Thus for each moment $m_{\rm k}$ (k = 1, ..., 18), we define

$$\chi^2_k = (\chi^2_{k,(a)} + \chi^2_{k,(b)})\,[1 - \Theta(m_k - M_k^{\rm min})\Theta(M_k^{\rm max} - m_k)] \tag{29}$$

with

$$\chi^2_{k,(a)} = \min(|M_k^{\rm min} - m_k|, |m_k - M_k^{\rm max}|)N_k^{-1}, \tag{30}$$

where $N_k = |M_k^{\rm min}|$ or $|M_k^{\rm max}|$, whether m_k lies on the left- or on the right-hand side of the corresponding sum-rule interval ($\chi^2_{\rm tot} = \sum_k \chi^2_k$) and

$$\chi^2_{k,(b)} = \begin{cases} 100, & 1 \le k \le 3 \\ 10, & 4 \le k \le 9 \\ 1, & 10 \le k \le 18\,. \end{cases} \tag{31}$$

The purpose of this parametrization (expressed in Eq. (31) in terms of arbitrary penalty points) is to ensure that third-order contributions should only *refine* the initial second-order representation of the distribution amplitude, and aid to suppress solutions with unphysical oscillations. Again we take refuge in the fact that we are formally dealing with a truncated expansion and we have to minimize the effect of unestimated higher-order corrections.

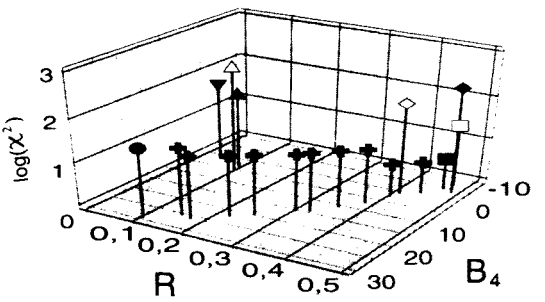

Fig. 5. Two-dimensional view of the "hierarchical" χ^2 criterion. Only the COZ branch of the "fiducial orbit" is shown.

Depending on the degree of matching with the corresponding sum rule, a solution found this way appears as a local minimum of the underlying χ^2 criterion (Fig. 5). A compilation of the spectrum of solutions, determined in [28, 51], is given in Table IV.

TABLE IV

Theoretical parameters defining the nucleon distribution amplitudes discussed in the text.

Model	B_1	B_2	B_3	B_4	B_5	ϑ[deg]	R	χ^2	Symbol
Het	3.4437	1.5710	4.5937	29.3125	−0.1250	−1.89	0.1040	33.48	•
Het′	4.3025	1.5920	1.9675	−19.6580	3.3531	24.44	0.4480	30.63	•
COZ^{opt}	3.5268	1.4000	2.8736	−4.5227	0.8002	9.13	0.4650	4.49	■
COZ^{up}	3.2185	1.4562	2.8300	−17.3400	0.4700	5.83	0.4881	21.29	+
COZ	3.6750	1.4840	2.8980	−6.6150	1.0260	10.16	0.4740	24.64	□
CZ	4.3050	1.9250	2.2470	−3.4650	0.0180	13.40	0.4870	250.07	♦
KS^{low}	3.5818	1.4702	4.8831	31.9906	0.4313	−0.93	0.0675	36.27	○
KS/COZ^{opt}	3.4242	1.3644	3.0844	−3.2656	1.2750	9.47	0.4530	5.66	○
KS^{up}	3.5935	1.4184	2.7864	−13.3802	2.0594	13.82	0.4820	40.38	○
KS	3.2550	1.2950	3.9690	0.9450	1.0260	2.47	0.4120	116.35	◇
GS^{opt}	3.9501	1.5273	−4.8174	3.4435	8.7534	80.87	0.0950	54.95	▲
GS^{min}	3.9258	1.4598	−4.6816	1.1898	8.0123	80.19	0.0350	54.11	▼
GS	4.1045	2.0605	−4.7173	5.0202	9.3014	78.87	0.0970	270.82	△
Samples									
0	3.3125	1.4644	3.1438	−1.0000	0.8750	7.67	.441	4.63	+
1	3.2651	1.4032	3.5466	2.8685	1.7954	8.94	.405	5.11	+
2	3.4026	1.4917	3.0629	7.3430	0.6719	8.75	.385	16.07	+
3	3.7225	1.5030	3.6592	10.7265	1.5154	9.29	.355	17.78	+
4	3.8407	1.4968	3.2142	14.4093	0.8757	10.49	.325	19.41	+
5	3.6544	1.4000	3.0993	15.5614	−0.1329	6.35	.305	18.15	+
6	3.8607	1.4000	3.2375	19.8571	−0.1635	6.32	.255	20.57	+
7	3.9783	1.4000	3.2706	22.4194	−0.4805	5.29	.225	21.69	+
8	4.1547	1.4000	3.3756	26.1305	−0.5855	5.02	.175	23.52	+
9	3.4044	1.5387	4.3094	25.5625	0.0625	.01	.153	30.80	+

Remarkably, it turns out that these nucleon distribution amplitudes can be organized across an "orbit" in the plane spanned by the Appell decomposition coefficient B_4 and the physical parameter R (Fig. 6), which is the ratio of the nucleon magnetic form factors: $R \equiv |G_M^n|/G_M^p$. This dynamical arrangement of sum-rule solutions ranges from COZ-like amplitudes (large R) to the novel heterotic solution (small R). The "metamorphosis" of solutions from one end of the orbit to the other end can be rigorously traced by interpolating solutions (notated "samples"). In the course of this analysis [28, 51], optimized versions with respect to the sum rules of all previous models have been determined. These amplitudes, denoted by the superscript "opt", are shown in Fig. 7. The important point, formally, is that this series of solutions can be continuously parametrized by a parameter, we termed "hybridity" angle, which is defined through the inner product

$$\vartheta = \arctan\left[\frac{\kappa_1(i)}{\kappa_2(i)}\right], \tag{32}$$

where $\kappa_1(i) = (\mathrm{GS}^{\mathrm{opt}}, i)$ and $\kappa_2(i) = (\mathrm{COZ}^{\mathrm{opt}}, i)$, and the index i denotes

collectively one of the nucleon distribution amplitudes listed in Table IV. The hybridity angle is based on the observation that $\mathrm{COZ}^{\mathrm{opt}}$ and $\mathrm{GS}^{\mathrm{opt}}$ are almost orthogonal to each other with respect to the weight of the nucleon-kernel eigenfunctions $w(x_i) = \Phi_{\mathrm{as}}(x_i)/120$. (Their normalized inner product yields 0.1607, which corresponds to an angle of 80.8°.) It provides a measure to quantify the mixing of geometric characteristics of amplitudes associated with different types of (asymmetric) momentum balance. Its utility lies in the fact that it relates amplitudes to each other, even if they do not belong to the "fiducial orbit". Turning to GS-type amplitudes, they correspond to local minima of χ^2 at considerably lower levels of accuracy and constitute an "island" which is separated from the "fiducial orbit" by a large χ^2 barrier. (For more details, we refer to [28, 51] and previous talks mentioned in the references.)

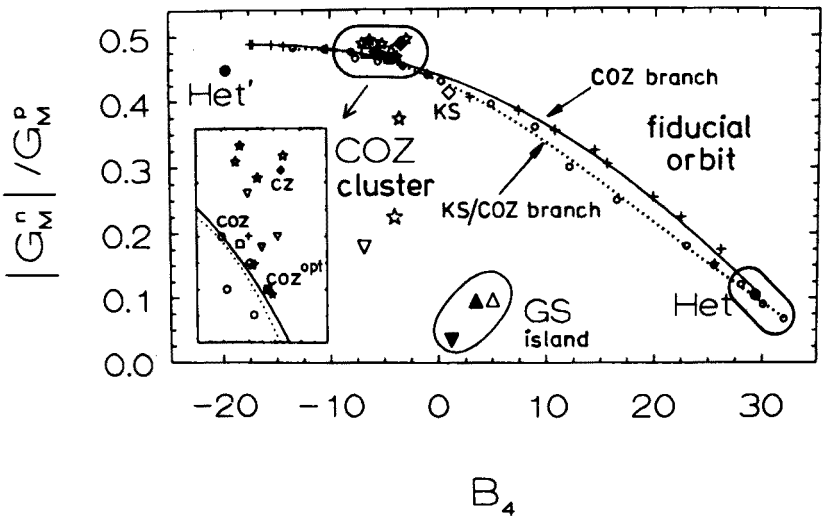

Fig. 6. Pattern of nucleon distribution amplitudes matching the COZ sum-rule constraints (crosses) and such to a combined set of KS/COZ sum rules (open circles). The inset at the lower left expands the vertical scale between 0.455 and 0.495 (corresponding to the B_4 interval $[-10, 0]$) to exhibit the close agreement between the "fiducial orbit" and a variety of proposed amplitudes with third-order Appell polynomials, not included in our analysis. Significantly, those model amplitudes which appear as isolated points are exactly the ones which possess unphysical features, namely, either in the form of spurious oscillations, or because they violate the RGE leading to a wrong QCD evolution behavior of form factors (see [28]).

Closing this section, we note that, following similar ideas of "heteroticity", we have combined the sum-rule approaches of Refs [43, 44] to derive an optimum distribution amplitude for the $\Delta^+(1232)$ isobar [46]. This amplitude, though similar in shape to the Carlson-Poor (CP) model amplitude [43], satisfies all sum-rule constraints derived by Farrar *et al.* (FZOZ) [44] while slightly violating only one of the (independent) CP-constraints (Table V). The profiles of our Delta distribution amplitudes plus those of Refs [43, 44] are shown in Fig. 8. The corresponding expansion coefficients B_n^{Δ} are given in Table VI.

TABLE V

Moments $n_1 + n_2 + n_3 \leq 3$ of model distribution amplitude for the Δ^+-isobar in comparison with the sum-rule constraints of Carlson and Poor (CP) [43] and Farrar, Zhang, Ogloblin, and Zhitnitsky (FZOZ) [44]. The numbers in parentheses are those given by FZOZ.

Moments	Sum rules	Models			
$(n_1 n_2 n_3)$	T_{Δ}(FZOZ)	CP	FZOZ	heterotic	FZOZ^{opt}
(000)	1	1	1	1	1
(100)	0.310–0.35	0.350	0.325 (0.32)	0.321	0.325
(001)	0.350–0.40	0.300	0.350 (0.36)	0.357	0.350
(200)	0.140–0.16	0.160	0.150	0.140	0.156
(002)	0.150–0.18	0.123	0.160	0.151	0.154
(110)	0.070–0.1	0.101	0.080 (0.07)	0.078	0.071
(101)	0.090–0.13	0.089	0.095 (0.1)	0.103	0.098
(300)	0.060–0.09	0.085	0.083 (0.085)	0.073	0.090
(003)	0.060–0.10	0.060	0.085 (0.081)	0.071	0.078
(210)	0.025–0.04	0.039	0.030 (0.025)	0.027	0.026
(201)	0.040–0.06	0.035	0.037 (0.04)	0.040	0.040
(102)	0.035–0.06	0.031	0.037 (0.039)	0.040	0.038
	V_{Δ}(CP)				
(001)	0.330–0.37	0.350	0.325	0.321	0.325
(002)	0.140–0.18	0.160	0.150	0.140	0.156
(101)	0.072–0.12	0.095	0.088	0.091	0.085

The amplitude notated FZOZ^{opt} — though compatible with the sum-rule constraints — seems to be in disagreement with the available data (see next section). This amplitude was obtained by demanding that the transition form factor G_M^*, calculated with the optimized version of the COZ nucleon distribution amplitude, is positive. This makes it apparent that optimum agreement with the (existing) sum rules *does not* automatically entail best agreement with the data, as we have stressed in [21].

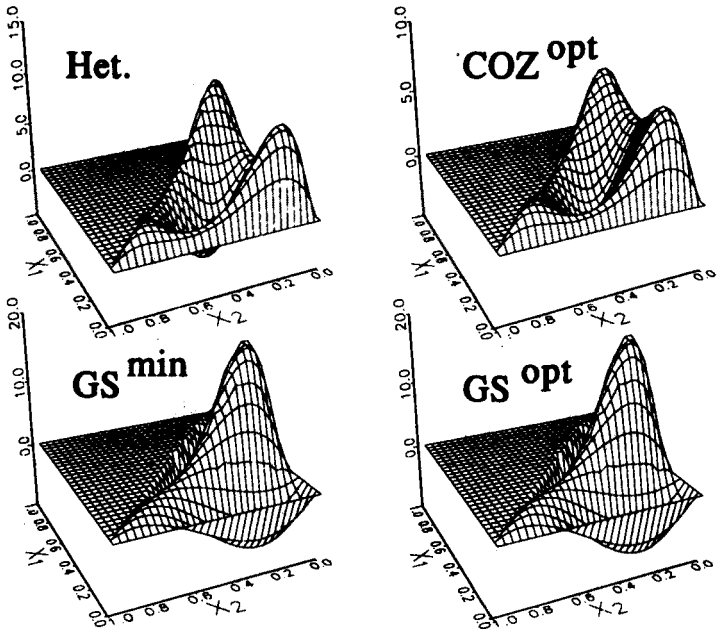

Fig. 7. Profiles of nucleon distribution amplitudes, commonly discussed in the literature.

TABLE VI

Expansion coefficients for Δ-isobar distribution amplitudes derived from QCD sum rules within a truncated expansion of eigenfunctions. Note that $B_0^{\Delta} = 1$ by normalization and that only eigenfunctions symmetric under $x_1 \leftrightarrow x_3$ contribute, i.e., $B_1^{\Delta} = B_4^{\Delta} \equiv 0$. As in the nucleon case, the notation of [29] is adopted.

	Models			
Expansion coefficients	CP	FZOZ	heterotic	FZOZ^{opt}
B_2^{Δ}	0.350	−0.175	−0.2499	−0.1750
B_3^{Δ}	0.4095	1.071	0.3297	1.4117
B_5^{Δ}	0.1755	−0.486	−1.6205	−1.6200

4. Phenomenological applications

Having acquired a reliable set of nucleon distribution amplitudes, we are able to discuss concrete applications.

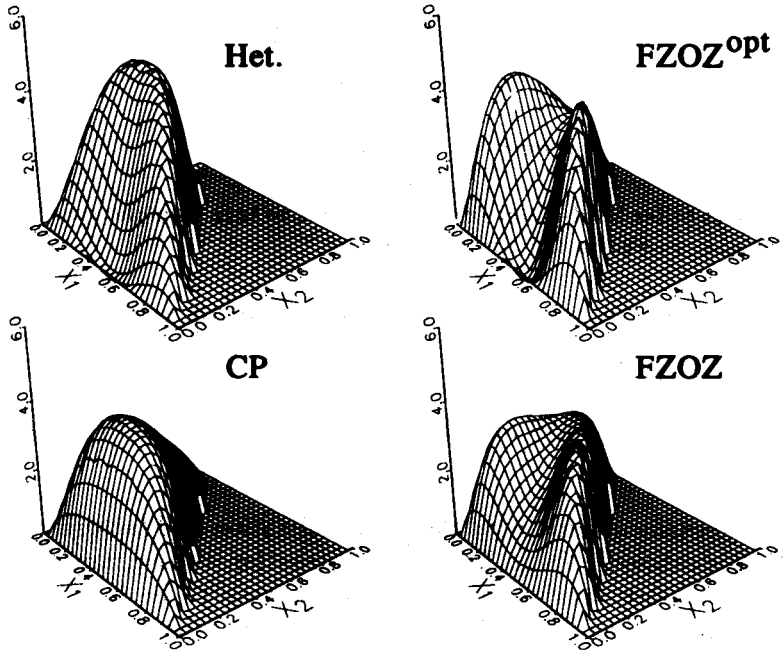

Fig. 8. Profiles of model distribution amplitudes for the Δ^+-isobar, derived from QCD sum rules.

The charge and magnetic form factors of the nucleon are "classical" observables to provide insight into the underlying quark-gluon substructure, as well as to connect to experimental data. To lowest order perturbation theory, the hard-scattering amplitude is the sum of all Feynman diagrams for which the three quark lines are connected pairwise by two gluon propagators (Fig. 9). This allows the quarks in the initial and final proton (neutron) to be viewed as moving collinearly up to transverse momenta of order μ. Then it is quite easy to show that $T_H \sim (\alpha_s(Q^2))^2/Q^4$, wherein $\alpha_s(Q^2)$ is the running coupling constant of QCD in the one-loop approximation.

The Pauli form factor F_2 and hence the electric form factor G_E cannot be calculated within such a hard scattering scheme, since they both require helicity-flip transitions which are not possible for (almost) massless quarks in the collinear approximation. These form factors are dominated by sizeable higher-twist contributions and their calculation demands additional nonperturbative input [52]. Taking the + component of the electromagnetic

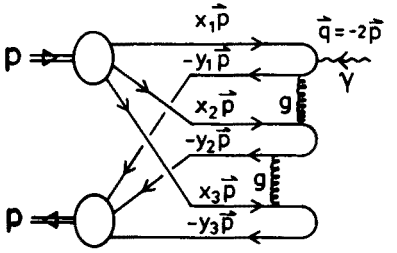

Fig. 9. Lowest order hard-gluon exchange needed to turn over the spectator quarks in the nucleon, viewed in the Breit frame.

vertex, the helicity-conserving part of the form factor is represented by

$$G_M(Q^2) = \int_0^1 [dx] \int_0^1 [dx'] |f_N(\mu)|^2 \, \Phi^\star(x',\mu) T_H(x,x',Q,\mu) \Phi(x,\mu)\,, \quad (33)$$

where for the sake of simplicity the renormalization and factorization scales have been identified. To go beyond perturbation theory, nonperturbative diagrams involving quark-gluon condensates have to be included. (For a review we recommend [53].) To leading twist (twist three), these additional diagrams include operators with dimensionality $d > 0$, giving rise to power corrections. Their contributions are incorporated in corresponding Wilson coefficients in the OPE, which in our case depend on the moment order $M = n_1 + n_2 + n_3$. Those of order $M = 3$ have been calculated in [26]; they have yet to be independently verified. Using these values and the analytical expressions derived in [29], the proton and neutron form factors can be calculated in terms of the expansion coefficients B_n. The results for all considered models are shown in Fig. 10 in comparison with existing data (see [37] and previous references cited therein). Note that the Q^2-evolution of the coefficients B_n has been neglected and that an average value $\bar{\alpha}_s(Q^2)$ outside the integral in Eq. (33) has been used (peak approximation). Here and below the values $\Lambda_{\rm QCD} = 180$ MeV [54] and $|f_N| = 5.0 \times 10^{-3}$ GeV^2 [25, 26] are used.

Since there are no direct data on G_M^n beyond, say, 5 GeV^2, it is virtually impossible to extract experimental values for the neutron form factors in a model-indepedent way. Therefore, we show in Fig. 10 the theoretical predictions along with G_M^n-data, extracted under the proviso of two extreme, albeit reasonable assumptions:

(i) assuming that the electric neutron form factor is at least of the order of the magnetic one (open circles), and

(ii) assuming $G_E^n = 0$ (black dots).

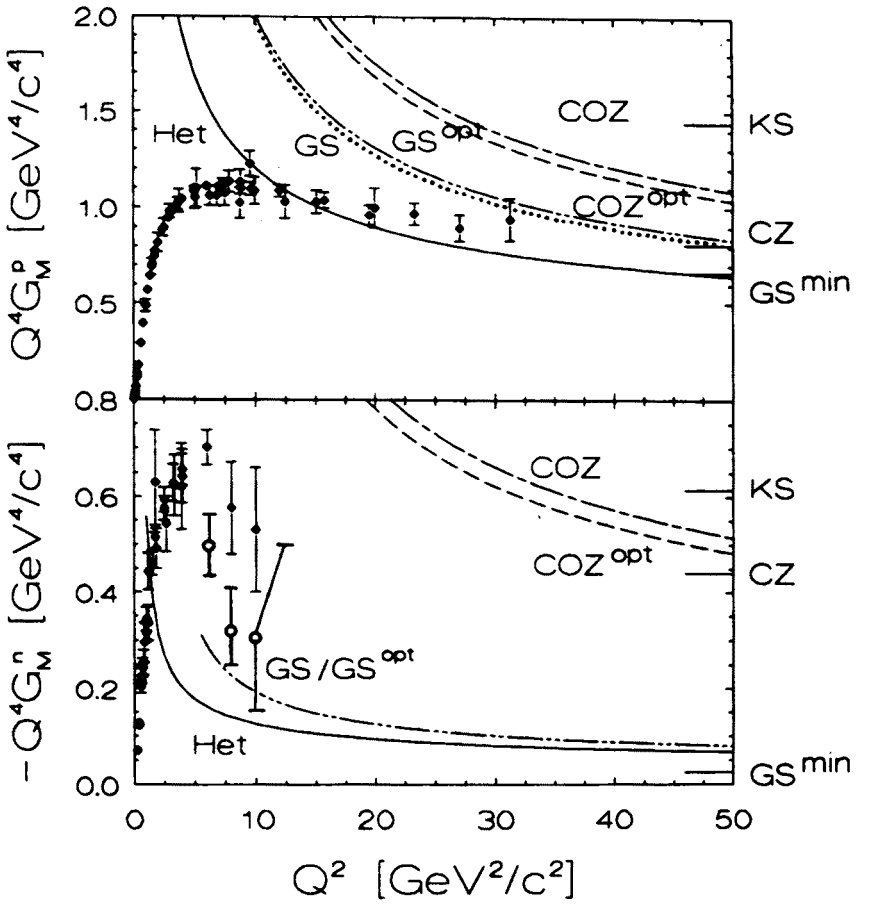

Fig. 10. Comparison with available data of the magnetic form factor of the proton and the neutron for different model distribution amplitudes.

Using the heterotic amplitudes for the nucleon [45] and the Δ^+-isobar [46], a similar good agreement with the data was found (Fig. 11). A recent re-analysis of the high Q^2 SLAC data by Stuart *et al.* [55] shows that the "heterotic" predictions are consistent with the data within the error bars, even in the simple peak approximation (lowest solid line). A refined treatment given in [46], which includes QCD evolution effects (dashed line), shows that the decrease of the form factor is consistent with a power-law behavior modified by logarithmic corrections due to anomalous dimensions, in agreement with perturbative QCD.

One observes from Figs 10, 11 that at low Q^2 the agreement between the calculated form factors and the data rapidly deteriorates because perturbation theory becomes increasingly inapplicable and the one-loop parametriza-

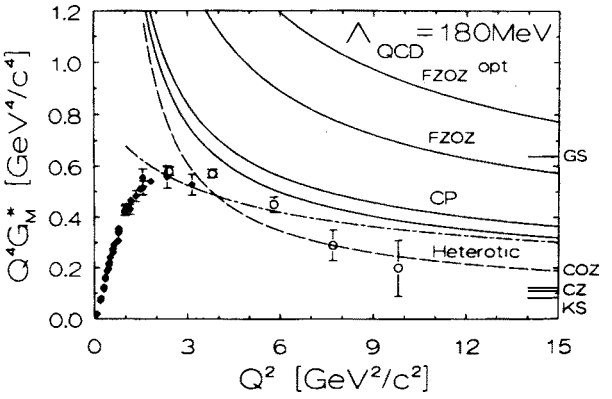

Fig. 11. Transition form factor $\gamma p\Delta^+$, calculated with the heterotic distribution amplitude for the nucleon and various Δ^+ distribution amplitudes in comparison with existing experimental data (see [46]). The dashed-dotted line shows a calculation [46] which takes into account a dynamical gluon mass to saturate α_s at low Q^2. Predictions from previous nucleon distribution amplitudes are indicated at the right margin. The open circles denote the data from Stuart's [55] analysis. Note that for all curves the value $|f_\Delta| = 11.5 \times 10^{-3}$ GeV^2 from [43] has been used.

tion of $\alpha_s(Q^2)$ becomes inadequate. It is clear that in this regime the perturbative predictions *should* not look like any data, since the *true* nucleon distribution amplitude receives contributions from all twists (*e.g.*, higher Fock-space components), contributions which are not accounted for in the formalism.

The last application we consider in the present work deals with exclusive decays of charmonium states to $p\bar{p}$. Such decays are sensitive to the nucleon distribution amplitude and hence may serve to discriminate proposed model distribution amplitudes. Calculations of charmonium decays have been performed by many authors (for references see [45]). Our own calculations follow those of Chernyak, Ogloblin, and Zhitnitsky [48]. We consider first the ${}^3P_J$ states with $J = 1, 2$. The branching ratio for the decay of the χ_{c1} state ($J^{PC} = 1^{++}$) into $p\bar{p}$ is given by

$$\mathrm{BR}\left(\frac{{}^3P_1 \to p\bar{p}}{{}^3P_1 \to \mathrm{all}}\right) \approx \frac{0.75}{\ln \frac{\bar{M}}{\Delta}} \frac{16\pi^2}{729} \left|\frac{f_N}{\bar{M}^2}\right|^4 M_1^2 , \tag{34}$$

where $\bar{M} \approx 2m_c \approx 3$ GeV and $\Delta = 0.4$ GeV (the last value from [56]). The nonperturbative content of (34) is due to f_N and the decay amplitude for the process ${}^3P_1 \to p\bar{p}$, denoted M_1, which involves Φ_N. Inputting

$$\Phi_N(x_i) = \Phi_{\mathrm{as}}(x_i)\left[(B_0 + B_2 - 5B_3 - 5B_5) + (B_1 + B_4)(x_1 - x_3)\right.$$

$$+(-3B_2+7B_3+7B_5)x_2+(4B_3+14B_5)x_1x_3$$
$$+(8B_3-\tfrac{4}{3}B_4+\tfrac{14}{3}B_5)x_1^2+(8B_3+\tfrac{4}{3}B_4+\tfrac{14}{3}B_5)x_3^2] \quad (35)$$

in connection with Table IV, the decay amplitude M_1 for each model is computed with an elaborate integration routine which properly takes account of contributions near singularities [24]. The results for different model distribution amplitudes are compiled in Table VII.

TABLE VII

Exclusive charmonium decays into $p\bar{p}$ for a variety of nucleon distribution amplitudes. The data are taken from [47]. The numbers in parentheses are those given in [48]. The poor accuracy of these values effects the superiority of our computational algorithms.

Models	$M(^3P_1 \to p\bar{p}) = M_1$	$M(^3P_2 \to p\bar{p}) = M_2$	$M(^3S_1 \to p\bar{p}) = M_0$
heterotic	99849.6	515491.2	13726.8
CZ	28310.4 (0.63×10^5)	246052.8 (2.87×10^5)	7545.6 (0.72×10^4)
COZ	53625.6 (0.88×10^5)	298123.2 (3.4×10^5)	8758.8 (0.79×10^4)
COZ^{opt}	55137.6	289728.0	8499.6
GS	26366.4	232632.0	928.8 (0.7×10^3)
GS^{opt}	19915.2	230659.2	986.4
GS^{min}	17193.6	210729.6	964.8
KS	94723.2 (1.35×10^5)	416937.6 (4.84×10^5)	11484.0 (1.15×10^4)
asympt.	20086.6 (0.2×10^5)	43099.2 (0.43×10^5)	1517.4 (0.14×10^4)
Observables	$\mathrm{BR}\left(\frac{^3P_1 \to p\bar{p}}{^3P_1 \to \mathrm{all}}\right)$ in %	$\mathrm{BR}\left(\frac{^3P_2 \to p\bar{p}}{^3P_2 \to \mathrm{all}}\right)$ in %	$\Gamma(^3S_1 \to p\bar{p})$ [eV]
heterotic	0.77×10^{-2}	0.89×10^{-2}	138.37
CZ	0.06×10^{-2}	0.20×10^{-2}	41.81
COZ	0.22×10^{-2}	0.30×10^{-2}	56.34
COZ^{opt}	0.23×10^{-2}	0.28×10^{-2}	53.07
GS	0.05×10^{-2}	0.18×10^{-2}	0.63
GS^{opt}	0.03×10^{-2}	0.18×10^{-2}	0.71
GS^{min}	0.23×10^{-3}	0.15×10^{-2}	0.68
KS	0.69×10^{-2}	0.59×10^{-2}	96.84
asympt.	0.03×10^{-2}	0.01×10^{-2}	1.69
E760	$(0.78 \pm 0.10 \pm 0.11) \times 10^{-2}$	$(0.91 \pm 0.08 \pm 0.14) \times 10^{-2}$	$(180 \pm 16 \pm 26)$

The analogous expression to (34) for the χ_{c2} state ($J^{PC} = 2^{++}$) has the form

$$\mathrm{BR}\left(\frac{^3P_2 \to p\bar{p}}{^3P_2 \to \mathrm{all}}\right) \approx 0.85(\pi\alpha_s)^4 \frac{16}{729}\left|\frac{f_N}{\bar{M}^2}\right|^4 M_2^2, \quad (36)$$

which is Eq. (20) of [48] with an obvious minor correction. The results for

the branching ratio of this process, shown in Table VII, have been calculated with $\alpha_s(m_c) = 0.210 \pm 0.028$ (see third paper of [56]).

Similar considerations apply also to the charmonium decay into $p\bar{p}$ of the level $^3S_1$ with $J^{PC} = 1^{--}$. The partial width of J/ψ (*i.e.*, χ_{c0}) into $p\bar{p}$ is defined by

$$\Gamma(^3S_1 \to p\bar{p}) = (\pi\alpha_s)^6 \frac{1280}{243\pi} \frac{|f_\psi|^2}{\bar{M}} \left| \frac{f_N}{\bar{M}^2} \right|^4 M_0^2 , \tag{37}$$

where f_ψ determines the value of the $^3S_1$-state wave function at the origin. Its value can be extracted from the leptonic width $\Gamma(^3S_1 \to e^+e^-) = (5.36 \pm 0.29)$ keV [50] via the Van Royen-Weisskopf formula. The result is $|f_\psi| = 409$ MeV with $m_{J/\psi} = 3096.93$ MeV. Then, using the same values of parameters as before, we obtain the results shown in Table VII. One sees from this table that the agreement between the predictions of the heterotic model and the recent high-precision data of the E760 experiment at Fermilab is excellent in all considered cases.

In a completely analogous way, one can calculate exclusive decays of (helicity-conserving) charmonium states in $\Delta\bar{\Delta}$. Theoretical predictions for the branching ratios and partial decay widths of the Delta distribution amplitudes discussed above are given in [46].

5. Recent theoretical developments

Although there has been a rather high level of phenomenological success in the description of various exclusive reactions, as discussed in some detail above, severe criticism has been raised by Isgur and Llewellyn-Smith [13], and Radyushkin [10] concerning the endpoint contributions to form factors and related observables. Specifically, it has been argued that most of the contributions to the pion and proton magnetic form factors are arising from the endpoint regions of the x integration, implying a concomitant breakdown of ordinary factorization and rendering a perturbative treatment useless. The dominance of endpoint regions becomes even more pronounced when asymmetric distribution amplitudes for the hadrons are used, as those derived from QCD sum rules. Indeed, excluding these regions, the perturbative contribution is reduced to only a few precent. This led the above authors to conclude that perturbative QCD becomes applicable at such large momentum transfer that there is actually no chance for experimental verification in the foreseen future.

However, recent theoretical developments due to Li and Sterman [57, 58] based on RG techniques [59], enable the rigorous treatment of the endpoint regions of exclusive reactions by taking into account Sudakov-type

form factors [60] that resum gluonic radiative corrections. As a result, soft-gluon exchanges between the colored lines during the hard scattering are suppressed by rapidly decreasing exponential factors which control the probability of soft-gluon radiation. Technically, this is achieved by retaining in the denominators of the hard-scattering amplitude the transverse momentum dependence of virtual particles. This introduces (after Fourier transformation) a transverse separation scale $b_\perp$ which plays an important role in rescaling the argument of the running coupling constant α_s whenever the virtuality of the gluon propagators (which involves the longitudinal momentum fractions x_i) becomes small. Moreover, as $b_\perp$ increases, the Sudakov exponential factors decrease, reaching zero at $b_\perp = 1/\Lambda_{\rm QCD}$. Thus, potentially dangerous α_s singularities are cancelled by Sudakov corrections providing a well-defined expression for the form factor. In the pion case, this is automatically accomplished by the interquark separation so that always when a Sudakov exponent depends on $x \to 0$, the other one depends on $1-x$ and drops rapidly to zero [57], without having to saturate α_s via additional phenomenological parameters, *e.g.*, an effective gluon mass. Fig. 12 shows such a calculation which also includes the intrinsic $k_\perp$-dependence of the pion wave function [61] for which a Gaussian form is assumed. The curves shown were evaluated for two different models of distribution amplitudes: the asymptotic wave function [17] (dotted line) and the Chernyak-Zhitnisky one [53] (solid line). The main conclusion to be drawn is that the perturbative contribution is self-consistent at experimentally accessible values of momentum transfers, although its magnitude is too small compared to the data.

As regards the proton form factor, the situation is more complicated because several transverse scales are involved and therefore a careful IR regularization is required. Recall that the IR cutoff is the factorization scale below which OPE becomes a poor approximation. It is understood that genuine nonperturbative momenta are implicitly accounted for in the proton wave function. In order to ensure IR protection, we have considered in [62] optional IR cutoff prescriptions and found that in order to avoid infinities, while still using the $\overline{\rm MS}$ scheme, one has to set all transverse interquark separations equal, and use the maximum one as the appropriate IR cutoff scale ("MAX" prescription):

$$\bar{b} \equiv \max\{b_1, b_2, b_3\} = \bar{b}_1 = \bar{b}_2 = \bar{b}_3 \,. \tag{38}$$

The quantities $\bar{b}_l$ are IR cutoff parameters, naturally related to, but not uniquely determined by the interquark separations b_l, so that different choices are possible. The particular advantage of our approach is that it not only suffices to protect the amplitudes from becoming singular, but it also yields a perturbative contribution to the form factor which saturates,

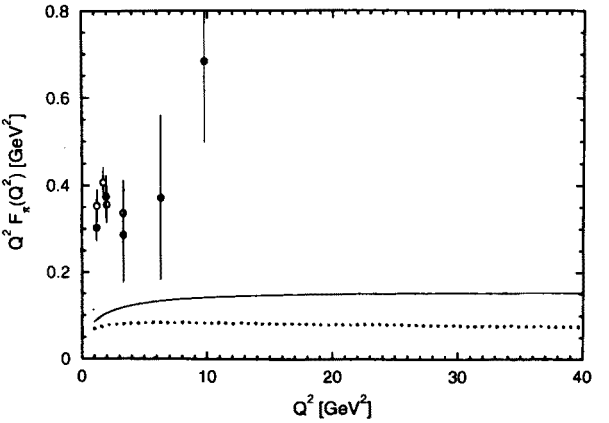

Fig. 12. The pion form factor in the spacelike region including Sudakov effects and those due to the intrinsic $k_\perp$-dependence of the pion wave function [61], evaluated for $\Lambda_{\rm QCD} = 200{\rm MeV}^2$. The data are taken from [65].

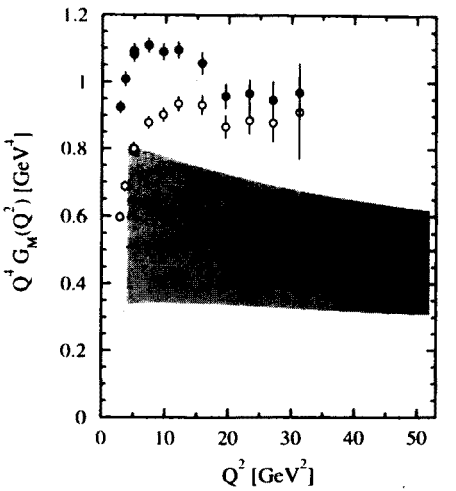

Fig. 13. Leading perturbative contribution to the proton magnetic form factor calculated within the modified convolution scheme, which takes into account gluonic radiative corrections via Sudakov-type form factors. The shadowed strip indicates the range of predictions derived from the set of nucleon distribution amplitudes shown in Fig. 6 and Table IV. The solid (dashed, dotted) line corresponds to the COZ (heterotic, COZ$^{\rm opt}$) distribution amplitude.

i.e., that it is rather insensitive to distances of order $1/\Lambda_{\rm QCD}$, thus rectifying Li's previous analysis. This means that the form factor accumulates its

main contribution in IR-safe regions. In particular, approximately 50% of the results are acquired in regions where $\alpha_s^2 \leq 0.54$ for momentum transfers starting at 6 to 10 GeV^2. The theoretical predictions for G_M^p, for the set of nucleon distributions accross the "fiducial orbit" and including QCD evolution, are shown in Fig. 13 (shaded band). Similar results have been obtained for the neutron [63]. Comparison of Figs 10 and 13 shows that the general effect of including Sudakov effects is a considerable reduction of the leading perturbative contribution. This effect is enhanced when the intrinsic $k_\perp$-dependence of the nucleon wave function is also taken into account. Full results and a detailed discussion of the numerical studies may be found in [62, 63].

6. Conclusions

We have reviewed a large body of exclusive reactions which relates to testing the validity of perturbative QCD, in particular factorization theorems, and the universality of nonperturbative hadron distribution amplitudes modeled on the basis of QCD sum rules. For instance, within the standard convolution scheme, the heterotic model successfully correlates a wide variety of unrelated observables to the data without tuning free parameters from case to case and without using additional phenomenological constraints. This agreement is non-trivial in the sense that there exist no other theories or models which fit the data nearly as well.

We have seen that IR sensitive contributions from endpoint regions are controllable within a modified convolution formalism which takes account of soft-gluon effects via Sudakov-type form factors leading to suppression of soft-gluon radiation at large quark separations. This Sudakov suppression provides sufficient IR protection of the perturbative treatment, ensuring its applicability at momentum transfers of present-day accelerators, at the expense that the magnitude of the leading perturbative contribution is reduced. Incorporation of confinement-size effects due to an intrinsic $k_\perp$-dependence [52] leads to further reduction. In light of these facts, we conclude that perturbative higher-order corrections giving rise to a rather large K-factor of the order of 2, as found for other large-momentum transfer processes [64], may be important. On the other hand, the sensitivity to the IR factorization scale is perhaps an indication for the importance of still unestimated higher-twist terms in the OPE. The examples presented in the last section may hopefully serve as an incentive to pursue further this course of investigations.

It is a pleasure to thank the organizers of the Zakopane School for their warm hospitality and the participants for stimulating discussions. Special thanks go to my close coworker Michael Bergmann for his invaluable contributions to the subject presented in this review.

REFERENCES

[1] M.A. Shifman, A.I. Vainshtein, V.I. Zakharov, *Nucl. Phys.* **B147**, 385, 448, 519 (1979).
[2] K.G. Wilson, *Phys. Rev.* **D10**, 2445 (1974).
[3] R. Gupta, *Acta Phys. Pol.* **B26**, No 1 (1995) in press.
[4] K. Goeke *et al.*, in Proceedings of the International Conference on Many Body Physics, Coimbra, Portugal, 1993, eds C. Fiolhais, M. Fiolhais, C. Sousa and C. Urbano, World Scientific, Singapore 1994, p. 73.
[5] D. Amati, R. Petronzio, G. Veneziano, *Nucl. Phys.* **B140**, 54 (1978); S. Libby, G. Sterman, *Phys. Rev.* **D18**, 3252 (1978); A.H. Mueller, *Phys. Rev.* **D18**, 3705 (1978); R. Ellis *et al.*, *Nucl. Phys.* **B152**, 285 (1979); A. Efremov, A.V. Radyushkin, *Teor. Mat. Fiz.* **42**, 167 (1980); **44**, 664, 774 (1981); *Phys. Lett.* **94B**, 245 (1980).
[6] K.G. Wilson, *Phys. Rev.* **179**, 1499 (1969).
[7] D.J. Gross, F.A. Wilczek, *Phys. Rev. Lett.* **30**, 1343 (1973); H.D. Politzer, *Phys. Rev. Lett.* **30**, 1346 (1973).
[8] G.P. Lepage, S.J. Brodsky, *Phys. Rev.* **D22**, 2157 (1980).
[9] A.V. Efremov, A.V. Radyushkin, *Riv. Nuovo Cimento* **3**, 1 (1980).
[10] A.V. Radyushkin, *Acta Phys. Pol.* **15**, 403 (1984).
[11] C.E. Carlson, J. Milana, *Phys. Rev.* **D44**, 1377 (1991).
[12] A.S. Kronfeld, B. Nižić, *Phys. Rev.* **D44**, 3445 (1991).
[13] N. Isgur, C.H. Llewellyn-Smith, *Phys. Rev. Lett.* **52**, 1080 (1984); *Nucl. Phys.* **B317**, 526 (1989).
[14] A.V. Radyushkin, in Particles and Nuclei, Proceedings of the Twelfth International Conference, Cambridge, Massachusetts 1990, eds J.L. Matthews *et al.*, *Nucl. Phys.* **A527** (Proc. Suppl.), 153c (1991); in Proceedings of the European Workshop on Hadronic Physics with Electrons Beyond 10 GeV, Dourdan, France, 1990, eds B. Frois and J.-F. Matthiot, *Nucl. Phys.* **A532** (Proc. Suppl.), 141c (1991); A.P. Bakulev, A.V. Radyushkin, *Phys. Lett.* **B271**, 223 (1991).
[15] A.B. Henriques, B.H. Kellet, R.G. Moorhouse, *Ann. Phys. (N.Y.)* **93**, 125 (1975).
[16] V.L. Chernyak, I.R. Zhitnitsky, *Nucl. Phys.* **B246**, 52 (1984).
[17] G.P. Lepage, S.J. Brodsky, *Phys. Lett.* **B87**, 359 (1979).
[18] A. Erdelyi *et al.*, *Higher Transcendental Functions*, McGraw-Hill, New York 1953, Vol. II.
[19] M. Peskin, *Phys. Lett.* **B88**, 128 (1979).
[20] Th. Ohrndorf, *Nucl. Phys.* **B198**, 26 (1982).

[21] N.G. Stefanis, M. Bergmann, in Proceedings of the Workshop on Exclusive Reactions at High Momentum Transfer, Elba, Italy, June 24–26, 1993, eds C.E. Carlson, P. Stoler, and M. Taiuti, World Scientific, Singapore 1994, p. 137 and p. 146.
[22] N.G. Stefanis, M. Bergmann, in Proceedings of the International Conference on Hadron Structure '93, Banská Štiavnica, Slovakia, September 5–10, 1993, eds S. Dubnička and A.Z. Dubničkova, Bratislava, Slovakia, 1994, p. 111.
[23] N.G. Stefanis, M. Bergmann, Proceedings of the Workshop on Quantum Field Theoretical Aspects of High Energy Physics, Kyffhäuser, Germany, September 20–24, 1993, eds B. Geyer and E.-M. Ilgenfritz, p. 112.
[24] M. Bergmann, Dissertation, Bochum University, 1994 (unpublished).
[25] I.D. King, C.T. Sachrajda, *Nucl. Phys.* **B279**, 785 (1987).
[26] V.L. Chernyak, A.A. Ogloblin, I.R. Zhitnitsky, *Z. Phys.* **C42**, 569 (1989).
[27] N.G. Stefanis, in 4th Hellenic School on Elementary Particle Physics, Corfu, Greece, September 2–20, 1992, eds E.N. Gazis, G. Koutsoumbas, N.D. Tracas, G. Zoupanos, Physics Department, National Technical University, Athens, Greece, Vol. II, p. 528.
[28] M. Bergmann, N.G. Stefanis, *Phys. Rev.* **D48**, R2990 (1993).
[29] N.G. Stefanis, *Phys. Rev.* **D40**, 2305 (1989); **D44**, 1616(E) (1991).
[30] D.G. Richards, C.T. Sachrajda, C.J. Scott, *Nucl. Phys.* **B286**, 683 (1987); G. Martinelli, C.T. Sachrajda, *Phys. Lett.* **B217**, 319 (1989).
[31] D. Daniel *et al.*, *Phys. Rev.* **D46**, 3130 (1992); M.C. Chu, M. Lissia, J.W. Negele, *Nucl. Phys.* **B360**, 31 (1991); R. Gupta, D. Daniel, J. Grandy, *Phys. Rev.* **D48**, 3330 (1993).
[32] M. Gari, N.G. Stefanis, *Phys. Lett.* **B175**, 462 (1986); *Phys. Rev.* **D35**, 1074 (1987).
[33] A. Schäfer, *Phys. Lett.* **B217**, 545 (1989).
[34] P.M. Stevenson, *Phys. Lett.* **B100**, 61 (1981); *Phys. Rev.* **D23**, 2916 (1981); *Nucl. Phys.* **B203**, 472 (1982); *Nucl. Phys.* **B231**, 65 (1984).
[35] R. Jakob *et al.*, *Z. Phys.* **A347**, 109 (1993).
[36] C.-R. Ji, A.F. Sill, R.M. Lombard-Nelsen, *Phys. Rev.* **D36**, 165 (1987).
[37] R.G. Arnold *et al.*, *Phys. Rev. Lett.* **57**, 174 (1986).
[38] S. Rock *et al.*, *Phys. Rev.* **D46**, 24 (1992).
[39] A. Lung *et al.*, *Phys. Rev. Lett.* **70**, 718 (1993).
[40] C.E. Carlson, M. Gari, N.G. Stefanis, *Phys. Rev. Lett.* **58**, 1308 (1987).
[41] C.E. Carlson, *Phys. Rev.* **D34**, 2704 (1986).
[42] C.E. Carlson, in Proceedings of the Workshop on Electronuclear Physics with Internal Targets, SLAC, Stanford University, Stanford, USA, January 5-8, 1987, eds R.G. Arnold and R. G. Minehart, p. 76.
[43] C.E. Carlson, J.L. Poor, *Phys. Rev.* **D38**, 2758 (1988).
[44] G.R. Farrar *et al.*, *Nucl. Phys.* **B311**, 585 (1988/89).
[45] N.G. Stefanis, M. Bergmann, *Phys. Rev.* **D47**, R3685 (1993).
[46] N.G. Stefanis, M. Bergmann, *Phys. Lett.* **B304**, 24 (1993).
[47] T.A. Armstrong *et al.*, *Nucl. Phys.* **B373**, 35 (1992).
[48] V.L. Chernyak, A.A. Ogloblin, I.R. Zhitnitsky, *Z. Phys.* **C42**, 583 (1989).

[49] J. Bonekamp, Diploma thesis, Bonn University, 1989 (unpublished).
[50] Particle Data Group, K. Hikasa *et al.*, *Phys. Rev.* **D45**, 1 (1992).
[51] M. Bergmann, N.G. Stefanis, *Phys. Lett.* **B325**, 183 (1994).
[52] P. Kroll, in Proceedings of the International Conference on Hadron Structure '93, Banská Štiavnica, Slovakia, September 5–10, 1993 eds S. Dubnička and A.Z. Dubničkova, Bratislava, Slovakia, 1994, p. 172.
[53] V.l. Chernyak, A.R. Zhitnitsky, *Phys. Rep.* **112**, 173 (1984).
[54] M.F. Gari, N.G. Stefanis, *Phys. Lett.* **B187**, 401 (1987).
[55] L. Stuart *et al.*, in Proceedings of the Workshop on Exclusive Reactions at High Momentum Transfer, Elba, Italy, JUne 24–26, 1993, eds C.E. Carlson, P. Stoler, M. Taiuti, World Scientific, Singapore 1994, p. 44.
[56] R. Barbieri, R. Gatto, R. Kögerler, *Phys. Lett.* **B60**, 183 (1976); R. Barbieri, R. Gatto, E. Remiddi, *Phys. Lett.* **B61**, 465 (1976); **B106**, 497 (1981).
[57] H.-N. Li, G. Sterman, *Nucl. Phys.* **B381**, 129 (1992).
[58] H.-N. Li, *Phys. Rev.* **D48**, 4243 (1993).
[59] J.C. Collins, D.E. Soper, *Nucl. Phys.* **B193**, 381 (1981); **B194**, 445 (1982); J.C. Collins, D.E. Soper, G. Sterman, *Nucl. Phys.* **B261**, 104 (1985).
[60] J. Botts, G. Sterman, *Nucl. Phys.* **B325**, 62 (1989).
[61] R. Jakob, P. Kroll, *Phys. Lett.* **B315**, 463 (1993); **B319**, 545(E) (1993).
[62] J. Bolz, R. Jakob, P. Kroll, M. Bergmann, N.G. Stefanis, *Z. Phys.* **C**, to be published.
[63] J. Bolz, R. Jakob, P. Kroll, M. Bergmann, N.G. Stefanis, *Phys. Lett.* **B**, to be published.
[64] N.G. Antoniou *et al.*, *Phys. Lett.* **B128**, 257 (1983).
[65] C.J. Bebek *et al.*, *Phys. Rev.* **D13**, 25 (1976); **D17**, 1693 (1978).